Acta Oceanol. Sin., 2017, Vol. 36, No. 11, P. 106–114
DOI: 10.1007/s13131-017-1141-9
http://www.hyxb.org.cn
E-mail: hyxbe@263.net

An automatic detection of green tide using multi-windows with their adaptive threshold from Landsat TM/ETM plus image

WANG Changying[1, 2, 3*], CHU Jialan[3, 4], TAN Meng[5], SHAO Fengjing[2], SUI Yi[2], LI Shujing[2]

[1] School of Data Science and Software Engineering, Qingdao University, Qingdao 266071, China

[2] Institute of Big Data Technology and Smart City of Qingdao, Qingdao 266071, China

[3] Key laboratory of Marine Red Tide Disaster Three-dimensional Monitoring Technology and Application, East China Sea Branch, State Oceanic Administration, Shanghai 200080, China

[4] National Marine Environmental Monitoring Center, State Oceanic Administration, Dalian 116023, China

[5] North China Sea Data and Information Service Center, North China Sea Branch, State Oceanic Administration, Qingdao 266061, China

Received 23 May 2016; accepted 29 July 2016

Abstract

Since the atmospheric correction is a necessary preprocessing step of remote sensing image before detecting green tide, the introduced error directly affects the detection precision. Therefore, the detection method of green tide is presented from Landsat TM/ETM plus image which needs not the atmospheric correction. In order to achieve an automatic detection of green tide, a linear relationship (y =0.723x+0.504) between detection threshold y and subtraction x (x=λ_{nir}–λ_{red}) is found from the comparing Landsat TM/ETM plus image with the field surveys. Using this relationship, green tide patches can be detected automatically from Landsat TM/ETM plus image. Considering there is brightness difference between different regions in an image, the image will be divided into a plurality of windows (sub-images) with a same size firstly, and then each window will be detected using an adaptive detection threshold determined according to the discovered linear relationship. It is found that big errors will appear in some windows, such as those covered by clouds seriously. To solve this problem, the moving step k of windows is proposed to be less than the window width n. Using this mechanism, most pixels will be detected $[n/k]\times[n/k]$ times except the boundary pixels, then every pixel will be assigned the final class (green tide or sea water) according to majority rule voting strategy. It can be seen from the experiments, the proposed detection method using multi-windows and their adaptive thresholds can detect green tide from Landsat TM/ETM plus image automatically. Meanwhile, it avoids the reliance on the accurate atmospheric correction.

Key words: automatic detection, green tide, adaptive threshold, Landsat TM/ETM plus image

Citation: Wang Changying, Chu Jialan, Tan Meng, Shao Fengjing, Sui Yi, Li Shujing. 2017. An automatic detection of green tide using multi-windows with their adaptive threshold from Landsat TM/ETM plus image. Acta Oceanologica Sinica, 36(11): 106–114, doi: 10.1007/s13131-017-1141-9

1 Introduction

Blooms of fast-growing macroalgae, sometimes referred to as "green tides", have been reported in many coastal areas all over the world (Merceron et al., 2007; Nelson et al., 2008; Ye et al., 2011; Smetacek and Zingone, 2013; Liu et al., 2013; Bao et al., 2015). Since 2007, large-scale green tides of *Ulva prolifera* have occurred each summer in the Yellow Sea (YS) and reached the coastline of Shandong Province, China (Hu et al., 2014; Zhang et al., 2015). Such macroalgal blooms—often associated with coastal eutrophication—frequently are detrimental to water-related human activities, such as tourism and aquaculture, and have multiple deleterious effects on natural ecosystems (Lyons et al., 2014; Zhou et al., 2015). Therefore, automatic monitoring green tide is one of the key technologies to understand the source, the geographic range and the drifting path. Satellite-derived remote sensing has the advantage of capturing and tracking large-sized patches. Many methods were proposed to detect the coverage area of the outbreak green tide, such as NDVI (normalized difference vegetation index), FAI (floating algae index) (Hu, 2009) and SAI (scaled algae index) (Keesing et al., 2011) methods. All these methods are under the assumption of accurate atmospheric correction, and the detection threshold is set to 0, then the higher is regarded as green tide, and the lower is regarded as sea water. In fact, due to the diversity of atmospheric conditions, and the impact of cloud covered, it is very difficult to achieve an accurate atmospheric correction. That is also the reason why these methods cannot achieve an automatic detection of green tide with high accuracy.

Therefore, this paper proposes an automatic method to detecting green tide from Landsat TM/ETM plus image, which needs not an atmospheric correction. First, the relationship between the detection threshold and the average brightness of the detected image will be discovered from massive detection samples; second, in order to improve the precision, a kind of co-

Foundation item: The National Natural Science Foundation of China under contract Nos 41506198 and 41476101; the Natural Science Foundation Projects of Shandong Province of China under contract No. ZR2012FZ003; the Science and Technology Development Plan of Qingdao City of China under contract No. 13-1-4-121-jch.
*Corresponding author, E-mail: wcing80@126.com

operative detection mechanism by multi-windows will be introduced; finally, the conclusions will be given.

2 Automatic detection of green tide from Landsat TM/ETM plus image

Based on China Oceanic Information Network (http://www.coi.gov.cn/gongbao/), we can see that green tide has occurred in June and July every year since 2008, especially in the coastal waters near Qingdao City, Shandong Province. At the same time, there were few other algae outbreaks in the area from the Environmental Status Bulletin. Therefore, this paper assumes that the algae disaster in this area in June and July must be green tide. Because the green tide occurred in the sea water, the land area will be masked firstly. Only the sub-image covering the seawater area is remained and used to detect the green tide. The study areas include the seas off China in an area of 34°–36°N, 119°–122°E in the red box in Fig. 1.

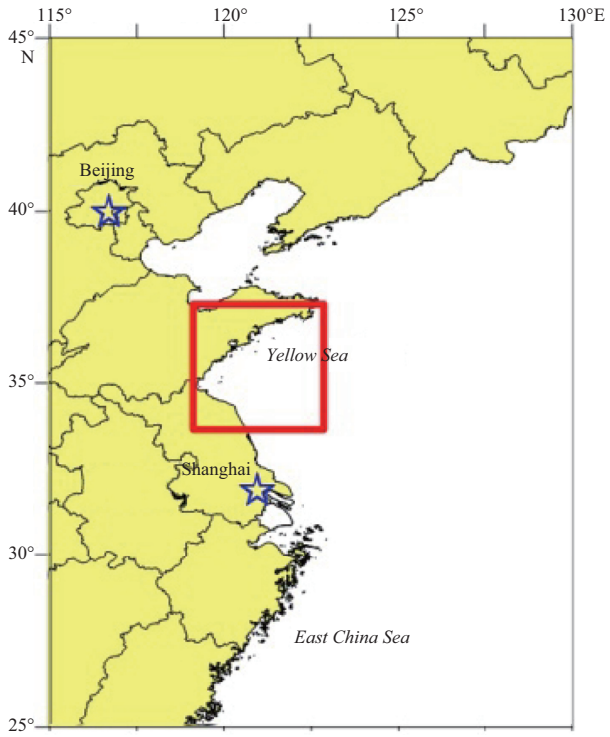

Fig. 1. Map with red box showing the study region of green tide.

2.1 *Correlation analysis between image brightness and detection threshold*

To realize detecting green tide from Landsat TM/ETM plus images automatically, the spectral values of the sea, the cloud and the green tide are anlyzed from the examples extracted from the Landsat TM image on June 22, 2009, as shown in Fig. 2.

It can be seen from Fig. 2, for the sea water samples, the average spectral value of Band 3 is slightly higher than that of Band 4; for green tide samples, the average spectral value of Band 3 is significantly lower than that of Band 4; but for the cloud samples, the average spectral value of Band 3 is also slightly higher than that of Band 4. That is consistent with the principle of the NDVI method.

In this paper, we use the following method to detect green tide.

For a pixel in a Landsat TM/ETM plus image, if it satisfies

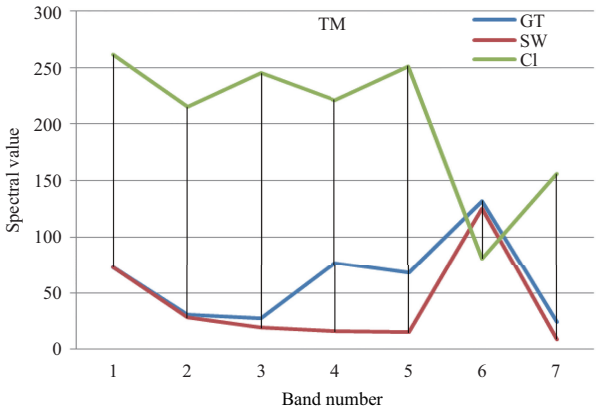

Fig. 2. Comparison of spectral values between green tide, sea water and cloud in Landsat TM/ETM plus image. GT represents green tide, SW sea water, and Cl cloud.

$\lambda_{nir}-\lambda_{red}>T$, it is classified as green tide; otherwise it is classified as sea water or cloud. Where T is about 0. Since the purpose of this paper is to detect green tide, sea water and cloud will not be distinguished.

In order to determine the detection threshold T automatically based on the image, the Landsat TM/ETM plus image on June 11 and 27, July 13 and 29, 2008, June 4 and 10, 2011 and July 15, 2012 were collected. Every landsat TM/ETM plus image was divided into many sub-images (also called windows) with size of 300 pixel×300 pixel firstly. Combined with historical observations from China Oceanic Information Network, the green tide range was detected from each sub-image by visual judgment, and the optimal detection threshold was obtained based on the principle as follow.

Figure 3a is a 300×300 pixel sub-image, Fig. 3b is the spectral subtraction of the near infrared band and the red band, and Figs 3c, d and e are the detection patches from sub-image Fig. 3a by using thresholds –7, –6, and –5, respectively. Considering the green tide patches often appeared piece by piece, large areas patches of green tide will be detected by this method. Therefore, the patches' area less than a pixel is regarded as noise. From Fig. 3c, it can be seen that there are many erroneous detection specks, especially on the upper and left corner of the image. The detections of Figs 3d and e agree well with the real situation. But the pixels' number is 1 286 while the detection threshold is –6, and that is 1 068 while the detection threshold is –5. In order to reduce the missing pixles, the optimal detection threshold is chosen as –6.

From the analysis of massive samples selected from the collected images, it is found that the detection thresholds have a linear relationship (Fig. 4) with the spectral subtraction between the near infrared band (Band 4) and the red band (Band 3), which is expressed as

$$T = 0.723(\lambda_{nir} - \lambda_{red}) + 0.504, \quad (1)$$

where T is the detection threshold, λ_{nir} is the average spectral value of near infrared band, and λ_{red} is the average spectral value of red band.

To validate the threshold determined automatically according to the discovered linear relationship, an image near Qingdao coast on June 22, 2009 is acquired and used to detect green tide.

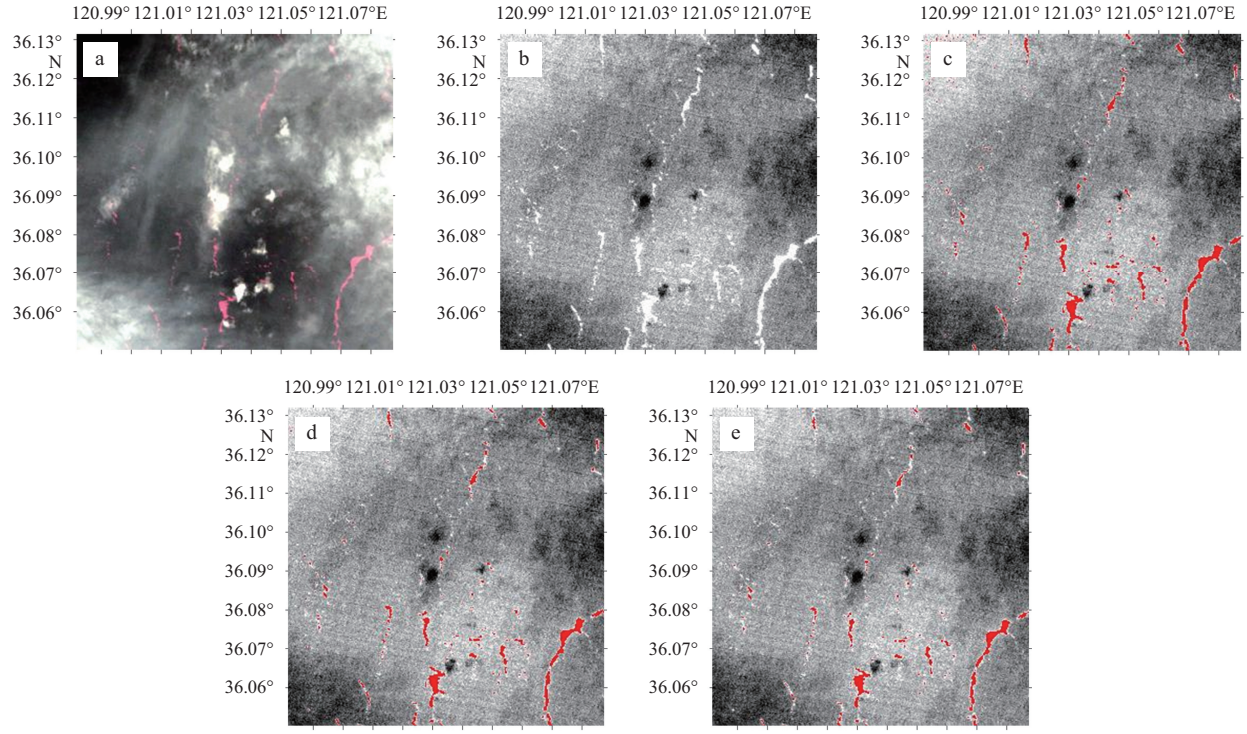

Fig. 3. Priciple of determining the optimum detection threshold. Figure 3a is Landsat TM false color composited sub-image to be detected (Bands 4, 3 and 2 for red, green and blue, respectively), Fig. 3b is subtraction image of the near infrared and the red bands, and Figs 3c, d and e are the detection results from the sub-image by using thresholds –7, –6, and –5, respectively.

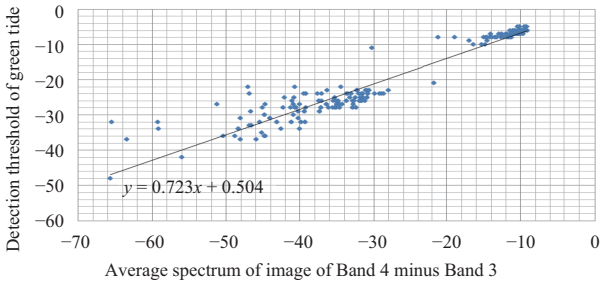

Fig. 4. Relationship between the detection threshold and substraction Band 4 minus Band 3.

The original image and the detected result are shown in Figs 5a and b, respectively. It is found that some patches are detected well (such as Regions 2 and 3), but others are not (such as Region 1) when a universal threshold was used. That is because the brightnesses of different areas are different in the image. Therefore, before detecting green tide, the image will be divided into many small sub-images (named windows). Then each sub-image will be detected using a partial threshold determined by Eq. (1) adaptively.

2.2 *Analysis of the optimal size of sub-image*

Because the brightness of different regions may be different in a Landsat image, one threshold cannot detect green tide with high accuracy everywhere. Therefore, the image will be divided into a plurality of windows (a window is a sub-image) with a same size firstly. For each window, a local threshold is determined adaptively to detect green tide. In order to find the optimum size of detecting window for most of the Landsat TM/ETM plus image, the images on June 11 and 28, 2008 and July 11, 2010 are collected and used to detect green tide by adaptive local thresholds in several sizes of windows. The experimental results are shown in Figs 6–8, where the horizontal axis is the row or column (the row is equal to the column) of the detecting window; the vertical axis is the number of the detected pixels; and the red line represents the number of pixels detected by visual interpretation.

From the experimental results, it is found that the window size between 500×500 pixels and 1 000×1 000 pixels is all appropriate. The small windows are suited for detecting small plaques, but the large ones are suited for detecting large ones. Moreover, the experiments show that the windows larger than 1 000×1 000 pixel can not detect a new region that did not detected by 500–1 000 windows.

From the detection results in Fig. 6, it is found that the pixels' numbers detected by 200×200, 400×400 and 800×800 pixels windows are much higher than the real situation. Similarly, from the detection results on June 28, 2008 (Fig. 7), the pixels' number detected by 1 300×1 300 pixels window is also much higher than the real situation; and the same situation appeares in the detction on July 11, 2010 (Fig. 8). That is because the adaptive detection threshold in some windows is not proper. There is an error detection while using an error threshold, just like the situation shown in Fig. 9. Therefore, we present a cooperative detection strategy by using multi-windows. Using this strategy, an individual error in a separate window can be ignored.

2.3 *Cooperative detection using multi-windows*

When the window size was set to a fixed value and the distance (we also called it sliding step) between two neighbouring windows was set to the window size, every pixel in the image would be detected only once. It would be pront to the false detec-

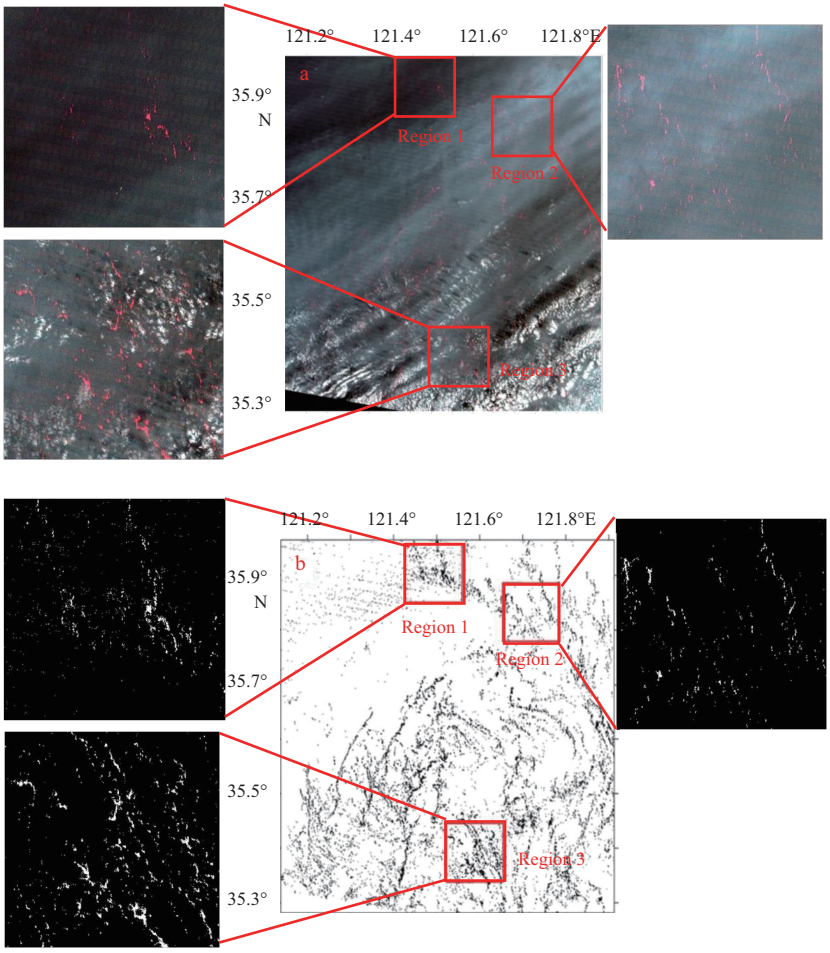

Fig. 5. Landsat TM false color composited image (Bands 4, 3 and 2 for red, green and blue, respectively) and the green tide detection results accquired on June 22, 2009.

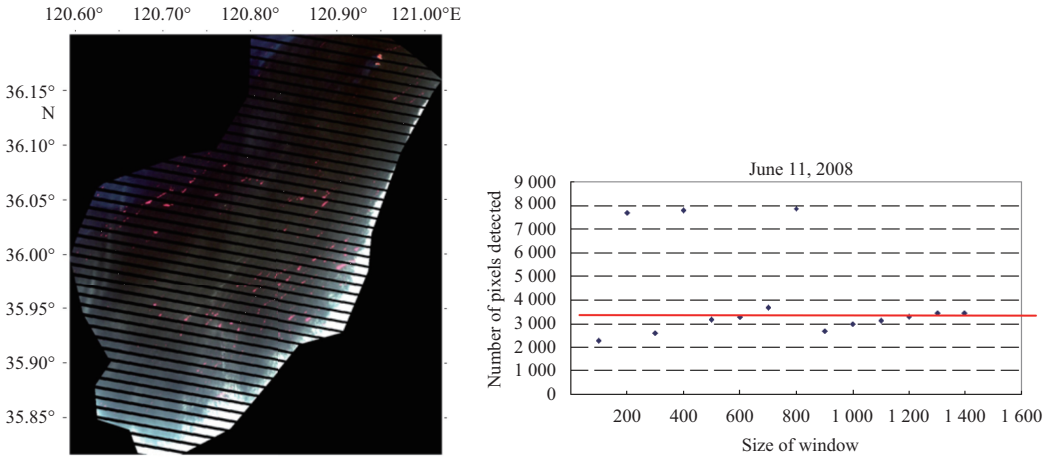

Fig. 6. Landsat TM/ETM plus image and the detection result of different windows on June 11, 2008.

tion while the window had a lower quality or was covered by cloud. To avoid this situation, this paper does not use n as the sliding step (n is the size of window) of the window during the detection by window of $n \times n$, but a value less than n. For example, if the window size is 500×500 pixels, and the sliding step is 100 pixels, most image pixels will be detected [500/100]×[500/100]=25 times except for the boundary pixels. Then, a "majority rule" voting mechanism will be used to assign the pixel to green tide or not. In order to determine how many votes can be the most effective, Landsat TM/ETM plus image on June 11, 2008 is collected and used to detect green tide, the window size is set from 500 to 1 200, the sliding step Δs is set to 100 and 200, respectively. The results are shown in Figs 10 and 11. The detected pixels' number of green tide by sliding step 100 is more than that by sliding step

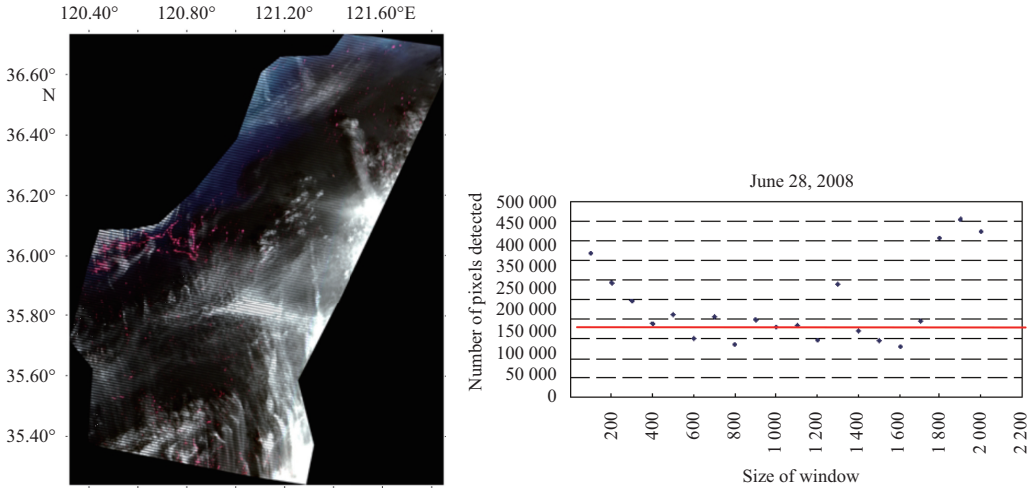

Fig. 7. Landsat TM/ETM plus image and the detection result of different windows on June 28, 2008.

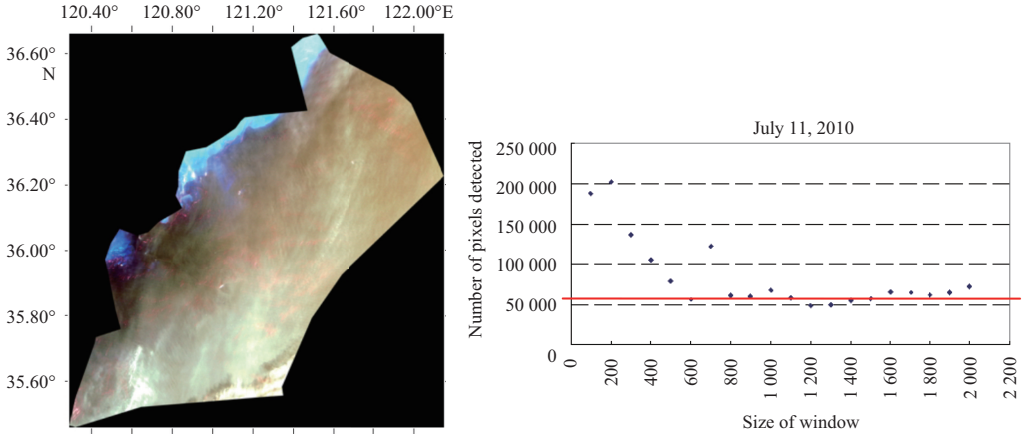

Fig. 8. Landsat TM/ETM plus image and the detection result of different windows on July 11, 2010.

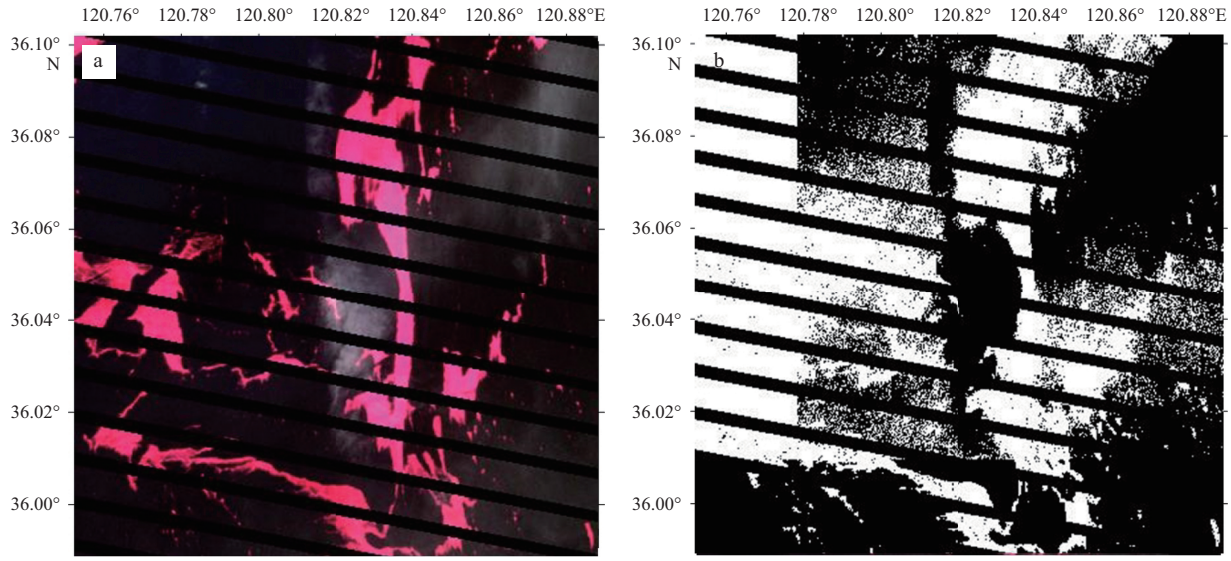

Fig. 9. Comparison of Landsat ETM plus false color composited image and detection result by 1 300×1 300 pixels window on June 28, 2008. a. Landsat ETM plus false color composited image, and b. detection result by 1 300×1 300 pixels window.

200. That is because every pixel is detected less when the sliding step is 200, for example, if the window is 600×600 pixels and the sliding step is 200 pixels, each pixel will be detected nine times at the most, but the boundary pixels will be detected even less. That

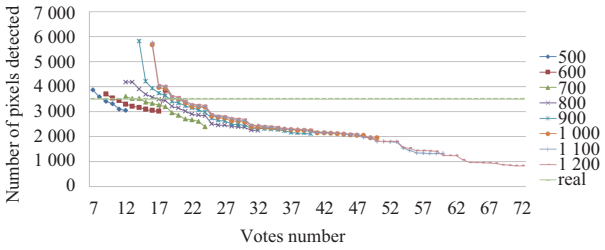

Fig. 10. The relationship between the detection and votes number when the window is from 500 to 1 200 and the sliding step is 100.

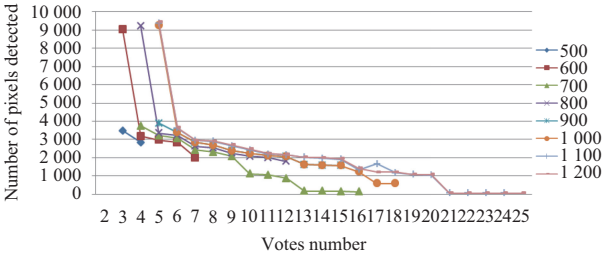

Fig. 11. The relationship between the detection and votes number when the window is from 500 to 1 200 and the sliding step is 200.

makes the boundary pixels miss easily. That is why the detection result by sliding step 200 was less than that by sliding step 100. Therefore, we choose the best sliding step as 100 pixels.

Through detection experiments from many images, it is found that the green tide detection results are related to the number of votes, which is shown in Fig. 12. While sliding step is 100, the optimal votes numbers of different windows are different, but they fluctuate within a certain range.

2.4 *Green tide detection using multi-windows collaboratively*

From our experiments, it was found that the small patches were often ignored while the window was large, and the large patches were often missed while the window was small. In order to play their advantages together, 600×600, 800×800 and 1 000×1 000 pixels windows are chosen to detect and vote the green tide pixels, respectively. The final detection result will be given by the

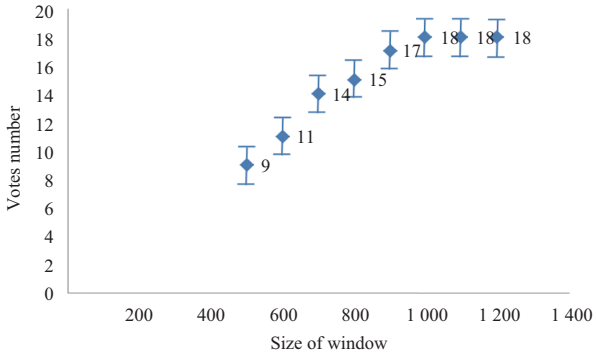

Fig. 12. The relationship between the window size and the number of votes.

union of the three detection results. In this way, the patches with different sizes will be detected with high precision, and automatic detection of green tide from Landsat images is realized. The flow chart of the adaptive threshold detection process by sliding window is shown in Fig. 13.

3 Results

In order to verify the automatic method for detecting green tide proposed in this paper, two Landsat ETM plus image on July 1, 2015 (without cloud) and June 24, 2016 (with thin cloud) are acquired and used to detect green tide, respectively. This paper selects four sub-images with four kinds of atmospheric and oceanic conditions for green tide detection, which are a region of deep water without cloud, a region of shallow water without cloud, a region of deep water with thin clouds and a region of shallow water with thin clouds, respectively. Then three methods (the proposed method, FAI and NDVI methods) are used to detect green tide from the four sub-images. The experiments results are shown in Figs 14–17. Figure 14 shows the false color composited sub-image of the region of shallow water with thin clouds and its detection results; Fig. 15 shows the false color composited sub-image of the region of deep water with thin clouds and its detection results; Fig. 16 shows the false color composited sub-image of the region of shallow water without cloud and its detection results; Fig. 17 shows the false color composited sub-image of the region of deep water without cloud and its detection results. An atmospheric correction is not needed by our pro-

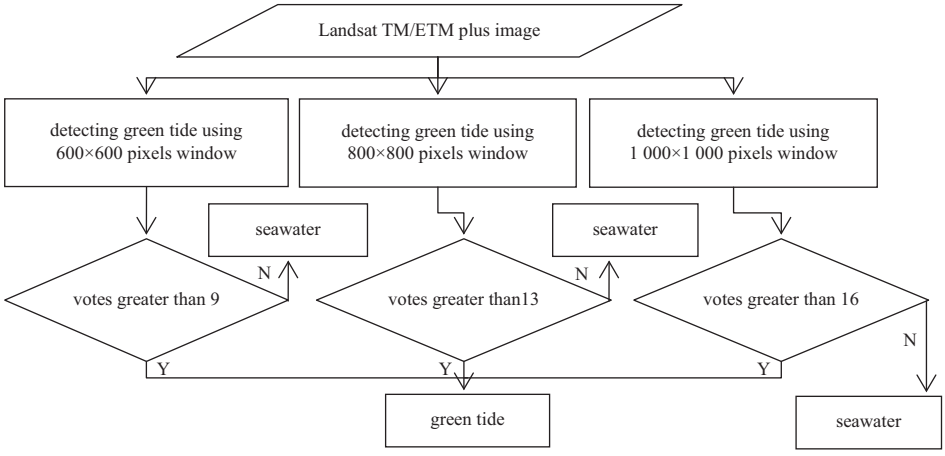

Fig. 13. Flow chart of the adaptive threshold detection method by multi-windows.

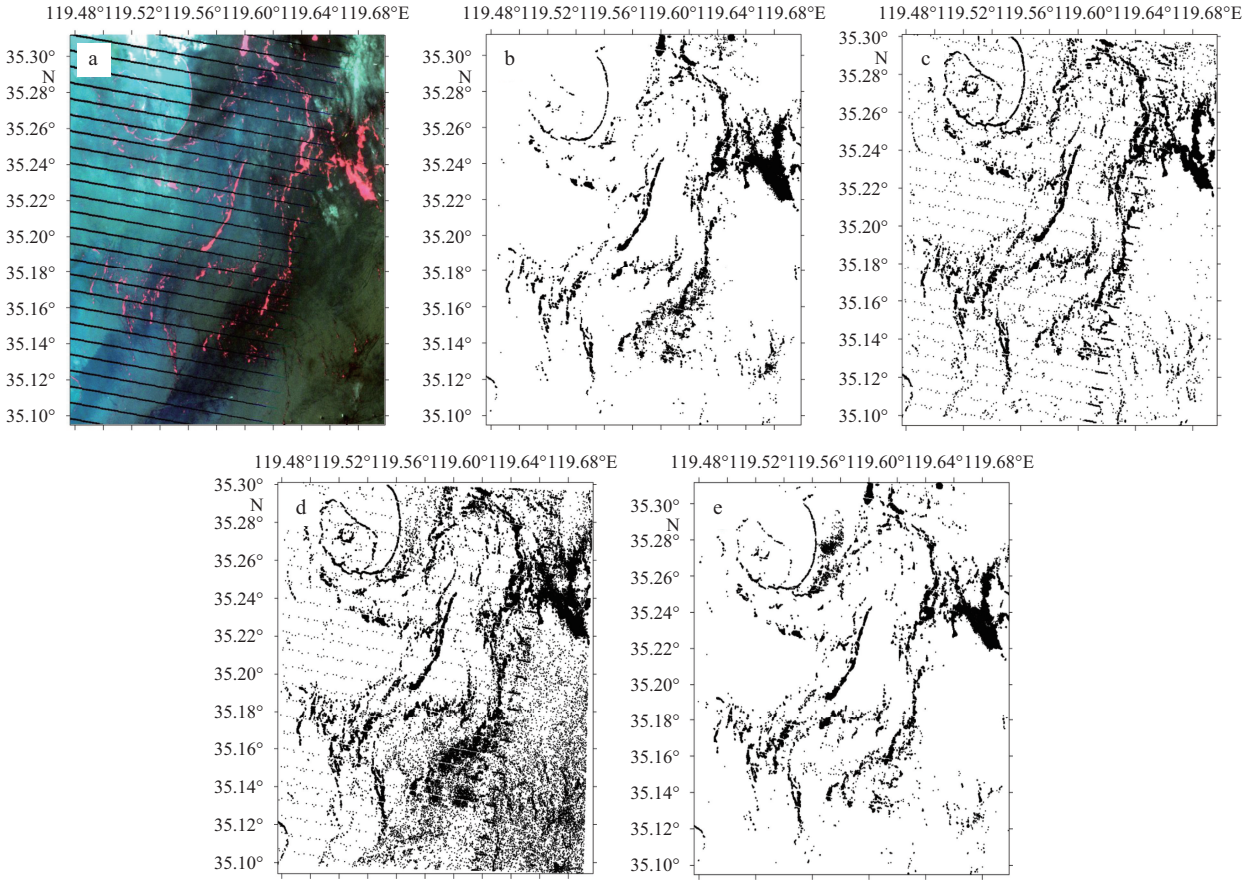

Fig. 14. Landsat ETM plus false color composited sub-image and the detections by our method, FAI method, NDVI method and artificial interpretation of coastal water region with thin cloud. a. Original image to be detected, b. the detection result using our method, c. the detection result using NDVI method, d. the detection result using FAI method, and e. the artificial interpretation by experts.

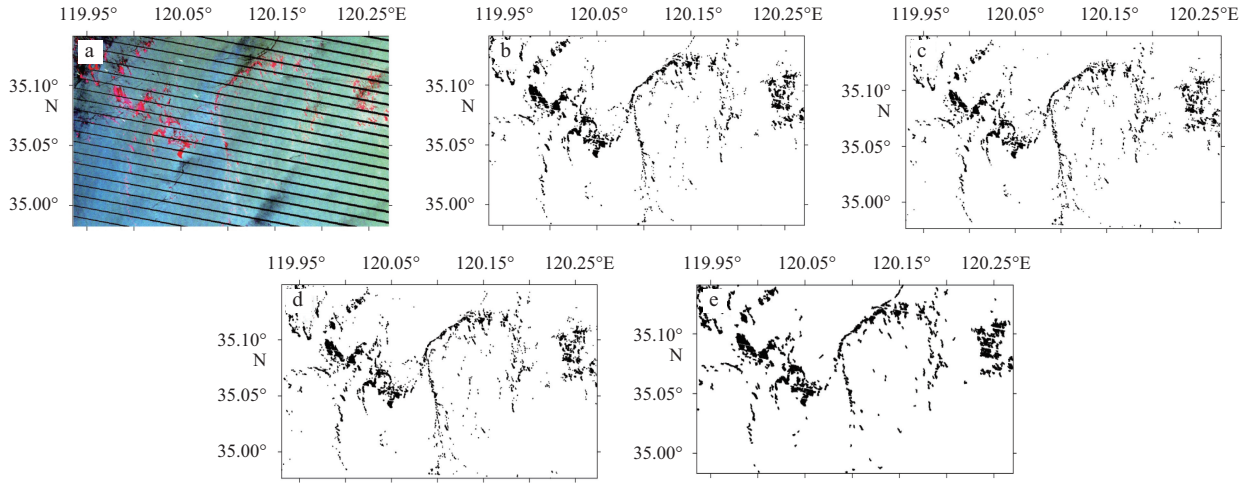

Fig. 15. Landsat ETM plus false color composited sub-image and the detections by our method, FAI method, NDVI method and artificial interpretation of deep water region with thin cloud. a. Original image to be detected, b. the detection result using our method, c. the detection result using NDVI method, d. the detection result using FAI method, and e. the artificial interpretation by experts.

posed method, but it is needed by the FAI and NDVI methods. So ENVI 5.0 is used to geometric correction and radiometric calibration firstly, then FLAASH atmospheric correction is used to correct the sub images before detecting green tide.

In order to compare the detection precision of the three methods, the green tide patches of the four sub-images are interpretated by experts. The number of pixels detected by our proposed method, FAI method, NDVI method and artificial interpretation are shown in Table 1. A detection rate and a missing rate are calculated by the detections of the three methods (Table 2).

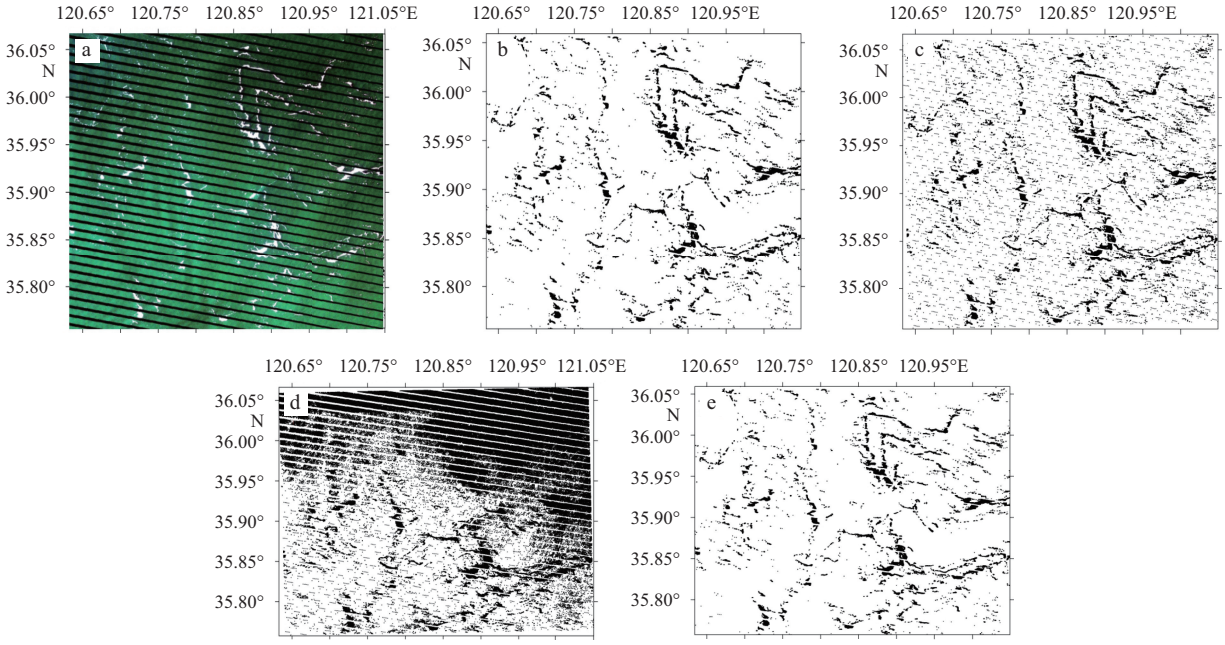

Fig. 16. Landsat ETM plus false color composited sub-image and the detections by our method, FAI method, NDVI method and artificial interpretation of coastal water region without cloud. a. Original image to be detected, b. the detection result using our method, c. the detection result using NDVI method, d. the detection result using FAI method, and e. the artificial interpretation by experts.

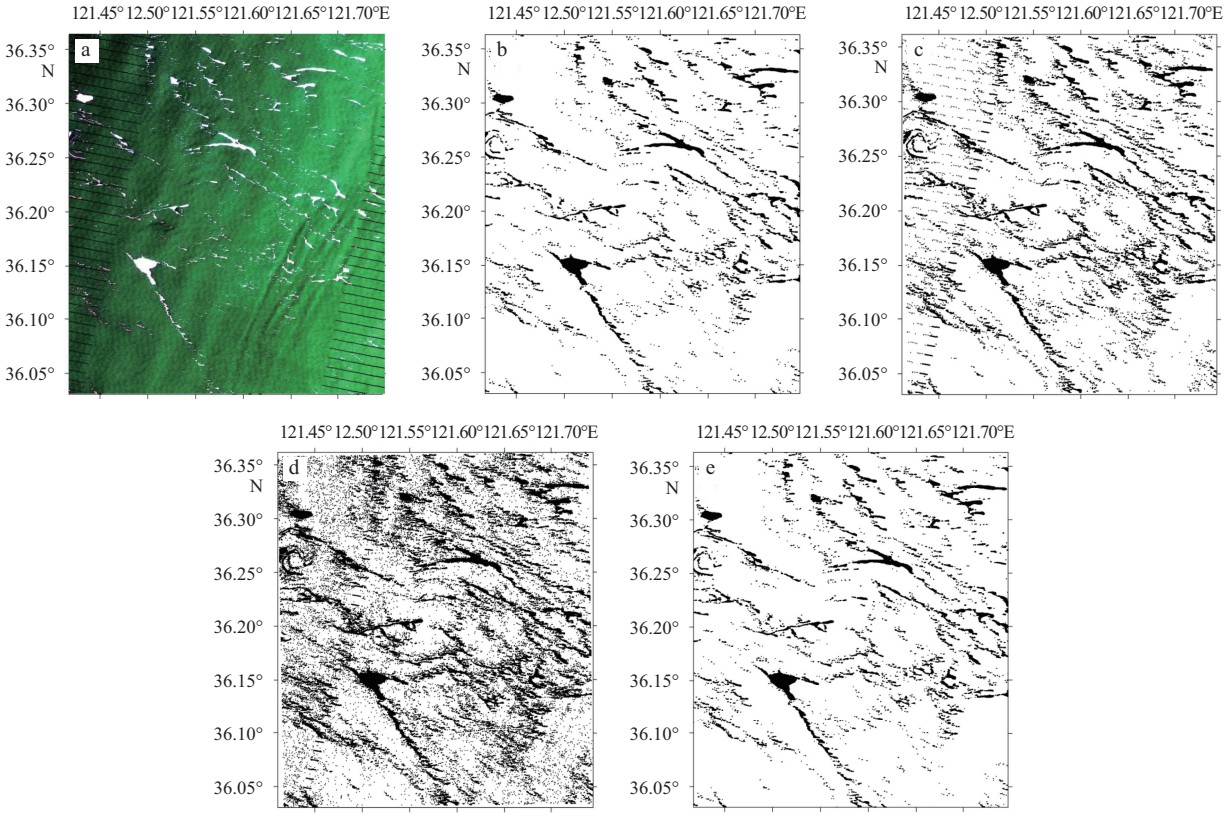

Fig. 17. Landsat ETM plus false color composited sub-image and the detections by our method, FAI method, NDVI method and artificial interpretation of deep water region without cloud. a. Original image to be detected, b. the detection result using our method, c. the detection result using NDVI method, d. the detection result using FAI method, and e. the artificial interpretation by experts.

Table 1. Green tide detections of our proposed method, FAI method, NDVI method and artificial interpretation

Environment		Our detection/pixels	FAI detection/pixels	NDVI detection/pixels	Actual detection/pixels
Deep water	no cloud	45 253	74 184	127 287	49 440
	thin cloud	15 159	15 883	16 794	21 756
Coastal water	no cloud	43 237	58 264	243 111	42 552
	thin cloud	24 612	34 796	56 704	24 479

Table 2. Detection rates and missing rates of our method, FAI method and NDVI method

Environment		Our method		FAI		NDVI	
		Detection rate/%	Miss rate/%	Detection rate/%	Miss rate/%	Detection rate/%	Miss rate/%
Deep water	no cloud	100	8.47	63.34	8.63	38.20	5.45
	thin cloud	96.13	5.21	81.34	9.67	76.51	8.35
Coastal water	no cloud	97.36	1.16	70.87	8.15	17.63	4.67
	thin cloud	90.65	3.27	86.32	7.23	72.45	4.31

Where the detection rate and the missing rate is calculated as follows:

Detection rate equals the number of correct detection pixels divided by the number of total detection pixels; missing rate equals subtraction of actual number of pixels minus the number of correct detection pixels divided by actual number of pixels.

It can be seen from the detections under the four kinds of atmospheric and oceanic conditions that the detection rate of our method is higher than those of the FAI and NDVI methods. Either way, there is some missing in the detections of the three methods. Their missing rates are close to each other and are all lower than 10%. The main reason of the low detection accuracy of the FAI and NDVI methods is that the detection results are dependent on the atmospheric correction results, and the error caused by the atmospheric correction seriously affects the green tide detection results. The method proposed in this paper does not need atmospheric correction, which obviously avoids the influence of the error introduced by the atmospheric correction, and it is also the main reason for the high accuracy of the proposed method.

4 Conclusions

This study tries to break through the conventional way of thinking (green tide detection from image after the atmospheric correction), and explores to find mechanism (green tide detection method) from noisy data (an image without the atmospheric correction). Normal thinking, before using remote sensing images for practical application, the atmospheric correction with high accuracy is needed, but this is a difficult goal. This paper regards green tide detection from Landsat image as an example to discuss if the atmospheric correction is necessary before application of remote sensing images. Therefore, this paper presents a green tide automatic detection method without the atmospheric correction. The method is not only suited for the region of deep water with thin cloud or without cloud, but suited for the region of shallow water with thin cloud or without cloud. Comparing with the FAI and NDVI detection results, it is shown that the detection accuracy of the proposed method under the situation of deep water and without cloud is the highest, and the accuracy for shallow water and thin cloud is lower. Even so, the detection rate can also reach more than 90%. At the same time, no matter under what kind of oceanic and atmospheric conditions, there also exists some missing, but the missing rate can be controlled below 10%.

The research results show that, with the massive accumulation of data, it is possible to discover the mechanism from the data, and it is more suitable for the information explosion era.

References

Bao Min, Guan Weibing, Wang Zongling, et al. 2015. Features of the physical environment associated with green tide in the southwestern Yellow Sea during spring. Acta Oceanologica Sinica, 34(7): 97–104

Hu Chuanmin. 2009. A novel ocean color index to detect floating algae in the global oceans. Remote Sensing of Environmen, 113: 2118–2129

Hu Song, Yang Hong, Zhang Jianheng, et al. 2014. Small-scale early aggregation of green tide macroalgae observed on the Subei Bank, Yellow Sea. Marine Pollution Bulletin, 81: 166–173

Keesing J K, Liu D Y, Fearns P, et al. 2011. Inter- and intra- annual patterns of Ulva prolifera green macroalgaes in the Yellow Sea during 2007–2009, their origin and relationship to the expansion of coastal seaweed aquaculture in China. Marine Pollution Bulletin, 62: 1169–1182

Liu D Y, Keesing J K, He P M, et al. 2013. The world's largest macroalgal bloom in the Yellow Sea, China: formation and implications. Estuar Coast Shelf Sci, 129: 2–10

Lyons D A, Arvanitidis C, Blight A J, et al. 2014. Macroalgal blooms alter community structure and primary productivity in marine ecosystems. Global Change Biology, 20: 2712–2724

Merceron M, Antoine V, Auby I, et al. 2007. In situ growth potenial of the subtidal part of green tide forming Ulva spp. Stocks. Since of The Total Environment, 384: 293–305

Nelson T A, Haberlin K, Nelson A V, et al. 2008. Ecological and physiological controls of species composition in green macroalgal blooms. Ecology, 89: 1287–1298

Smetacek W, Zingone A. 2013. Green and golden seaweed tides on the rise. Natrue, 504: 84–88

Ye Naihao, Zhang Xiaowen, Mao Yuze, et al. 2011. "Green tides" are overwhelming the coastline of our blue planet: taking the world's largest example. Ecological Research, 26: 477–485

Zhang Qingchun, Liu Qing, Yu Rencheng, et al. 2015. Application of a fluorescence in situ hybridization (FISH) method to study green tide in the Yellow Sea. Estuarine, Coastal and Shelf Science, 163: 112–119

Zhou Mingjiang, Liu Dongyan, Donal M, et al. 2015. Introduction to the special issue on green tides in the Yellow Sea. Estuarine, Coastal and Shelf Science, 163: 3–8